

# A Molecular Dynamics Study of Aqueous Solutions

## X. First Results for a NaCl Solution with a Central Force Model for Water

P. Bopp\*, W. Dietz, and K. Heinzinger

Max-Planck-Institut für Chemie (Otto-Hahn-Institut), Mainz, Germany

Z. Naturforsch. **34a**, 1424–1435 (1979); received October 25, 1979

The central force model for water has been employed in a molecular dynamics simulation of a 2.2 molal NaCl solution. The structural properties of the solution obtained are compared with results of previous simulations where the ST2 model of water was used. Preliminary results on the influence of the ions on the water molecule geometry in the hydration shells are reported. The spectral densities calculated from the hydrogen velocity autocorrelation functions by Fourier transformation indicate differences in the librational and vibrational frequencies between bulk water and hydration water of  $\text{Na}^+$  and  $\text{Cl}^-$ .

### I. Introduction

Computer simulations of aqueous electrolyte solutions have so far been performed with rigid models for the water molecule. The pair potentials for water-water and ion-water interactions in the Monte Carlo (MC) studies of alkali halide solutions by Beveridge et al. [1] were derived from ab initio calculations of Clementi and coworkers [2, 3]. In the molecular dynamics (MD) studies of various alkali halide solutions [4] and an  $\text{NH}_4\text{Cl}$  solution [5] reported in previous papers of this series the ST2 model of water [6] was used. It was the main disadvantage of these water models that the influence of the ions on the water molecule geometry and on the intramolecular vibrations could not be studied.

In this paper preliminary results of a MD study of an aqueous NaCl solution are reported where the basic periodic cube contained 200 oxygen and 400 hydrogen atoms which bear fractions of an elementary charge as well as 8 sodium and 8 chloride ions equivalent to a 2.2 molal solution. The water molecule geometry is solely preserved by an appropriate choice of the oxygen-hydrogen and hydrogen-hydrogen pair potentials which are taken from the latest version of the central force (CF) model of water [7], originally developed by Lemberg and Stillinger [8]. The ion-oxygen and ion-hydrogen pair potentials have been derived from ab initio calculations of Kistenmacher, Popkie and Clementi [9], while the ions are modelled as Lennard-Jones

(LJ) spheres with an elementary charge in the center.

In the present paper the structural properties of the solution obtained with the CF model for water are compared in detail with the results of an MD simulation of a NaCl solution where the ST2 model was employed [10] and with results from the MD simulation of pure CF water [7]. The geometry of the water molecules and the spectral densities of librations and vibrations have been calculated separately for the three kinds of water in the NaCl solution — bulk water, hydration water of  $\text{Na}^+$  and  $\text{Cl}^-$  — and differences are discussed. The results presented — at least as far as the dynamical properties of the solution are concerned — have to be considered preliminary as the simulation comprised only 3500 time steps equivalent to a total elapsed time of 1.4 picoseconds and because of deficiencies in the CF model.

### II. Effective Pair Potentials and Details of the Calculations

The complete set of the ten pair potentials employed in the MD simulation of the 2.2 molal NaCl solution is given in the Appendix.  $V_{\text{HH}}$ ,  $V_{\text{OH}}$ , and  $V_{\text{OO}}$  [Eqs. (A.1)–(A.3)] are those used in the MD simulation of pure CF water by Stillinger and Rahman [7]. The sodium and the chloride ion are described as before [10] by a LJ sphere with one elementary charge in the center. Equations (A.4) to (A.6) show the resulting pair potentials. The ion-water pair potentials — separated into four contributions  $V_{\text{NaO}}$ ,  $V_{\text{NaH}}$ ,  $V_{\text{ClO}}$ , and  $V_{\text{ClH}}$ , consistent with the central force model — are derived from the ab initio calculations of Kistenmacher, Popkie

\* Present address: Chemistry Department, University of California, Irvine, California 92717, USA.

Reprint requests to Dr. K. Heinzinger, Max-Planck-Institut für Chemie, Saarstr. 23, P.O.B. 3060, D-6500 Mainz.

0340-4811 / 79 / 1200-1424 \$ 01.00/0. — Please order a reprint rather than making your own copy.



Dieses Werk wurde im Jahr 2013 vom Verlag Zeitschrift für Naturforschung in Zusammenarbeit mit der Max-Planck-Gesellschaft zur Förderung der Wissenschaften e.V. digitalisiert und unter folgender Lizenz veröffentlicht: Creative Commons Namensnennung-Keine Bearbeitung 3.0 Deutschland Lizenz.

Zum 01.01.2015 ist eine Anpassung der Lizenzbedingungen (Entfall der Creative Commons Lizenzbedingung „Keine Bearbeitung“) beabsichtigt, um eine Nachnutzung auch im Rahmen zukünftiger wissenschaftlicher Nutzungsformen zu ermöglichen.

This work has been digitalized and published in 2013 by Verlag Zeitschrift für Naturforschung in cooperation with the Max Planck Society for the Advancement of Science under a Creative Commons Attribution-NoDerivs 3.0 Germany License.

On 01.01.2015 it is planned to change the License Conditions (the removal of the Creative Commons License condition "no derivative works"). This is to allow reuse in the area of future scientific usage.

and Clementi [9]. Each of the four pair potentials were chosen to consist of a Coulomb, a  $1/r^2$  and an exponential term. The coefficient of the Coulomb term is — as in Eqs. (A.1)—(A.6) — simply the product of the model charges involved. The ions bear one elementary charge while in the CF model 0.32983 *e* are assigned to the hydrogen atoms and consequently —0.65966 *e* to the oxygen atoms. The coefficients of the  $1/r^2$  and the exponential term have been determined in the following way: Clementi *et al.* calculated for various water molecule orientations and various ion-oxygen distances the total binding energy for the Na<sup>+</sup>-water complex [9a] and the Cl<sup>−</sup>-water complex [9b]. Then they obtained by a fit procedure an analytical expression for each of the two complexes which gives the binding energy solely as a function of ion-water-point charge distances (Eq. (B.1) in [9c]), where a rigid planar water model with six point charges was employed. Now, the Coulomb terms for various distances and water molecule orientations were subtracted from these expressions and the coefficients wanted were determined by a fit to the energy differences obtained in this way. The resulting pair potentials are given in Eqs. (A.7)—(A.10).

In Fig. 1 the pair potentials for Na<sup>+</sup>-water and Cl<sup>−</sup>-water from (A.7)—(A.10) are shown as a function of ion-oxygen distance for a coplanar arrangement with the ion-oxygen vector bisecting the HOH angle and the gas phase water molecule geometry ( $R_{OH} = 0.96$  Å;  $\angle HOH = 104.5^\circ$ ). The dots and circles indicate the binding energies for the ion-water complexes resulting directly from the *ab initio* calculations [9a, b]. The rather poor agreement for this orientation is a consequence of the fact that the best fit is achieved for all possible water molecule orientations. Additionally, the pair potentials with use of the ST2 model are drawn as dashed lines for comparison. It is interesting to note that the combination of the ST2 model, with the simple model for Na<sup>+</sup> and Cl<sup>−</sup> — a LJ sphere with an elementary charge in the center — leads to pair potentials not too different from the ones obtained from the *ab initio* calculations.

With an experimental density of 1.08 g/cm<sup>3</sup> for the 2.2 molal NaCl solution a side length of the basic cube of 18.42 Å resulted. The equations of motion were solved with a simplified version of the predictor-corrector algorithm described by Schäfer and Klemm [11] and employed for the MD simula-

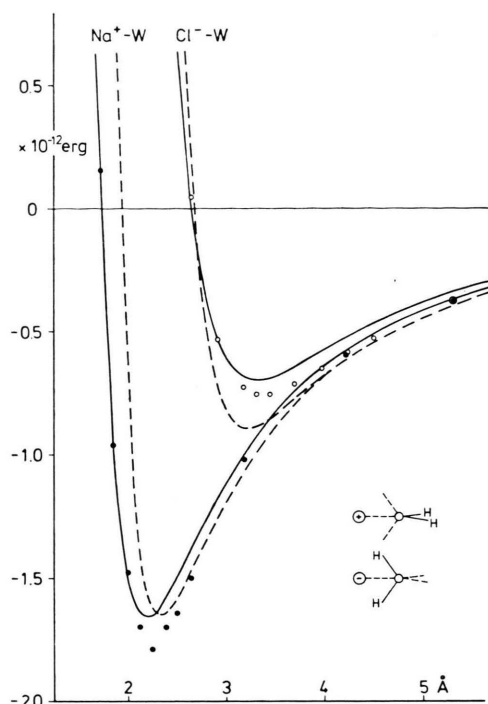


Fig. 1. Ion-water pair potentials as a function of ion-oxygen distance for the water molecule orientations shown in the insertion and for a geometry of the isolated water molecule with  $R_{OH} = 0.96$  Å and  $\angle HOH = 104.5^\circ$ , calculated from Eqs. (A.7)—(A.10). The dashed line results if the ST 2 water model is employed [10] and dots and circles indicate the binding energies from the *ab initio* calculations [9a, b].

tion of molten KCl. For the far ranging Coulomb interactions an Ewald summation was used similar to that described by Rahman, Stillinger and Lemberg [12]. The run from which the following results were derived extended over 3500 time steps equivalent to a total elapsed time of 1.4 picoseconds. The total energy showed a small downward trend amounting to about 30/00 over the whole run. The velocities were not rescaled during the simulation in order to get useful velocity autocorrelation functions. In this way the average temperature of the simulation was 290 K. The configuration with which this simulation was started was taken from a previous simulation of a NaCl solution with the ST2 model.

### III. Structural Properties

The ion-oxygen and ion-hydrogen radial distribution functions (RDF) are shown in Fig. 2 for the sodium ion and in Fig. 3 for the chloride ion

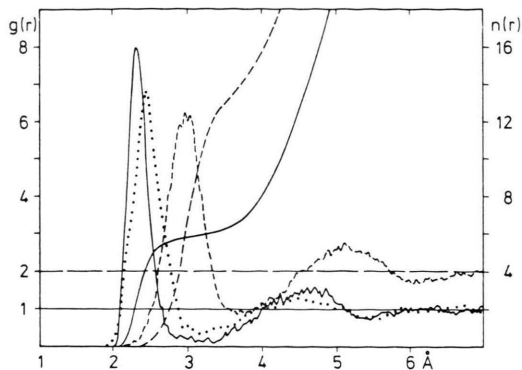


Fig. 2. Sodium-oxygen (full) and sodium-hydrogen (dashed) radial distribution functions and running integration numbers for a 2.2 molal NaCl solution with the central force model for water. The dotted line shows  $g_{\text{NaO}}(r)$  from a simulation with the ST2 model [10].

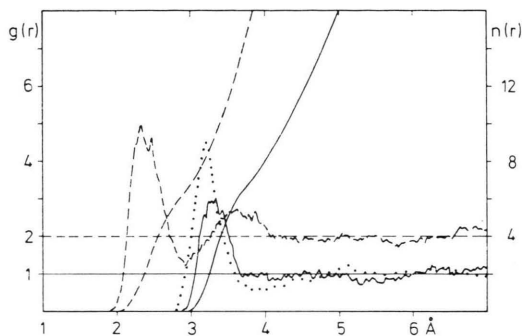


Fig. 3. Chloride-oxygen (full) and chloride-hydrogen (dashed) radial distribution functions and running integration numbers for a 2.2 molal NaCl solution with the central force model for water. The dotted line shows  $g_{\text{ClO}}(r)$  from a simulation with the ST2 model [10].

together with the corresponding running integration numbers  $n(r)$ . Additionally, the  $g_{\text{IO}}(r)$  from a simulation of a 2.2 molal NaCl solution with the ST2 model of water [10] are drawn as dotted lines in both figures for comparison. In going from the CF to the ST2 model the maxima of the first peaks in the ion-oxygen RDF's are shifted by 0.1  $\text{\AA}$  to larger distances for  $\text{Na}^+$  and smaller ones for  $\text{Cl}^-$ . This shift is expected from the pair potentials shown in Fig. 1 because it has been found in previous simulations that the first maxima in  $g_{\text{IO}}(r)$  almost coincide with the minima of the ion-water pair potentials for the energetically most favorable orientations. The difference in the heights of the first peaks in  $g_{\text{ClO}}(r)$  reflects the difference in the depth of the minima of the pair potentials. Therefore one might expect in  $g_{\text{NaO}}(r)$  — besides the shift in

the maximum — very similar first peaks, but they differ in height and width. This difference results most probably from the different orientations of the water molecules in the hydration shell of  $\text{Na}^+$  between CF and ST2 water as shown in Fig. 9 and discussed below. It should be mentioned that the position and the height of the first maxima in  $g_{\text{NaO}}(r)$  and  $g_{\text{ClO}}(r)$  agree very well with the results of the MC study of Beveridge *et al.* [1] who employed — as in this work — ion-water pair potentials derived from the *ab initio* calculations of Clementi and coworkers. As the best available data on ion-water binding energies (dots and circles in Fig. 1) are positioned in between the pair potentials calculated with the CF and ST2 model it might be expected that the correct  $g_{\text{NaO}}(r)$  and  $g_{\text{ClO}}(r)$  are somewhere in between the CF and ST2 curves in Figs. 2 and 3.

The hydration numbers — defined as the integral over  $g_{\text{IO}}(r)$  up to the first minimum:  $n(r_{\text{m1}})$  — have been found to be 5.9 and 8.4 for  $\text{Na}^+$  and  $\text{Cl}^-$ , respectively (the value for  $\text{Cl}^-$  is an upper limit because the first minimum of  $g_{\text{ClO}}(r)$  is not well defined as can be seen from Figure 3). From the simulation with the ST2 model the corresponding values 6.1 and 7.9 have been derived [10].

The oxygen-oxygen RDF for the 2.2 molal NaCl solution calculated with the CF model is compared in Fig. 4 with results from the simulation with the ST2 model. The main difference is the existence of a pronounced second maximum and second minimum in the case of the CF model. This far ranging structure leads to significantly better agreement with the structure function determined from an x-ray investigation of the NaCl solution [10] in the

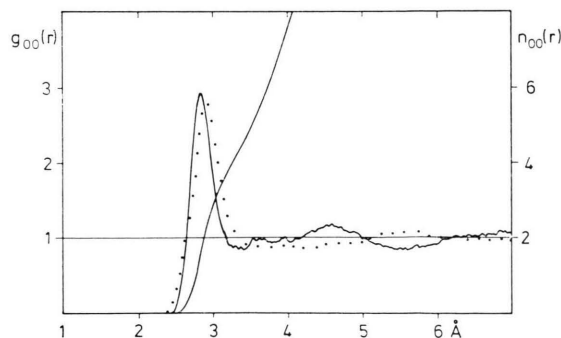


Fig. 4. Oxygen-oxygen radial distribution function and running integration number in a 2.2 molal NaCl solution with the central force model for water. The dotted line shows  $g_{\text{OO}}(r)$  from a simulation with the ST 2 model [10].

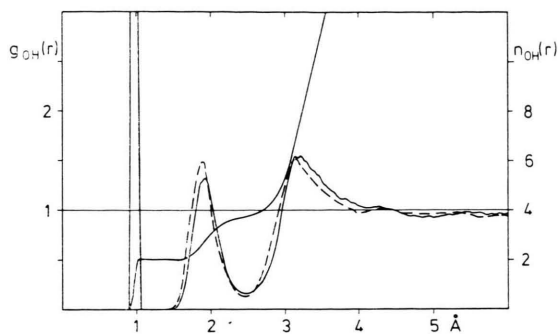


Fig. 5. Oxygen-hydrogen radial distribution function and running integration number in a 2.2 molal NaCl solution with the central force model for water. The dashed line shows  $g_{OH}(r)$  for pure CF water [7].

range of the double peak as shown in Fig. 11 and discussed in detail below. The comparison with pure CF water (Fig. 2 in [7]) shows that the first peak is slightly lower and the first minimum is less pronounced in the solution, an effect which has also been found in previous simulations with ST2 water. The number of nearest neighbors is difficult to compare as in both curves in Fig. 4 the first minimum is not well defined.

The oxygen-hydrogen RDF together with the running integration number  $n_{OH}(r)$  is shown in Figure 5. For comparison  $g_{OH}(r)$  for pure CF water — taken from Fig. 3 of [7] — is drawn additionally. The position of the first peak, the integral of which is exactly two, results from the intramolecular O—H distance. Its average value is 0.97 Å compared with 0.96 Å for pure CF water [7]. The intramolecular O—H distance has been calculated separately for bulk water and the hydration water of  $\text{Na}^+$  and  $\text{Cl}^-$ . A difference has not been found in the limits of error. In the hydration water of  $\text{Cl}^-$ , where preferentially a linear hydrogen bond is formed with the ion (see below), the O—H bond directed towards the ion can be treated separately from the second one. Again, a difference in the length of the two bonds has not been found. The second peak in  $g_{OH}(r)$  which describes the O—H distances to the hydrogen bonded neighboring water molecules is slightly lower in the solution than in pure CF water, a consequence of the disturbance of the water structure through the ions.

The hydrogen-hydrogen RDF shown in Fig. 6 is very similar to the one for pure CF water as far as can be judged from Fig. 4 in [7]. Only the first peak at about 1.5 Å — the intramolecular H—H distance

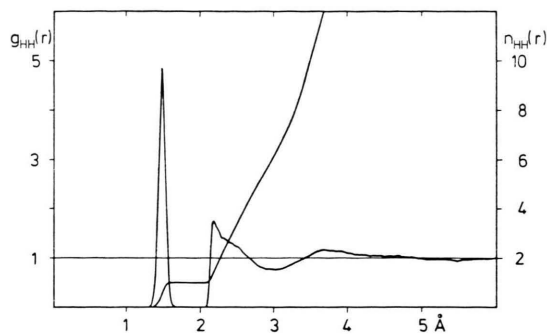


Fig. 6. Hydrogen-hydrogen radial distribution function and running integration number in a 2.2 molal NaCl solution with the central force model for water.

— seems to be shifted slightly to smaller distances in the solution and somewhat higher and narrower. This might be connected with differences in the HOH angle which has been calculated separately for bulk water, hydration water of  $\text{Na}^+$  and  $\text{Cl}^-$ . While the distributions of this angle are very similar for both kinds of hydration water, the difference between bulk water and hydration water seems to be significant. It is shown in Fig. 7 for bulk water and hydration water of  $\text{Na}^+$ . The average values — marked on the abscissa — have been calculated to be 99.9°, 99.3° and 99.4° for bulk water, hydration water of  $\text{Na}^+$  and  $\text{Cl}^-$ , respectively. The value for pure CF water could not be deduced with sufficient accuracy from the information given in [7]. The decrease in the HOH angle of the water molecules in the hydration shell of  $\text{Na}^+$  results from the repulsive forces exerted from the ion on the hydrogens and the attractive ones on the oxygen. In the case of the chloride ion, where the orientation of the water molecules is reversed (see below), analogous arguments lead also to a smaller angle of the hydration water relative to bulk water.

As the O—H distance is the same for all three kinds of water in the limits of uncertainty the decrease in the HOH angle leads to a small increase in the dipole moment of the water molecules in the hydration shells. Values of 1.98, 2.00 and 1.99 D have been found for bulk water, hydration water of  $\text{Na}^+$  and  $\text{Cl}^-$ , respectively. The isolated water molecule in the CF model has a dipole moment of 1.86 D.

The orientation of the water molecules in the hydration shells of the ions, which can be deduced from the relative positions of the maxima in  $g_{IO}(r)$  and  $g_{IH}(r)$  as shown in Figs. 2–3, is shown in more



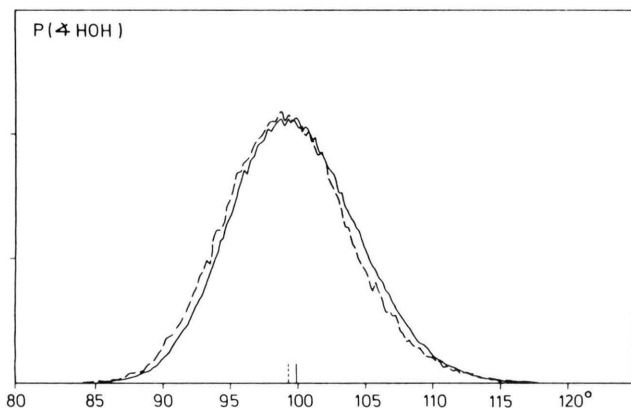


Fig. 7. Normalized distributions of the HOH angle for bulk water and hydration water of  $\text{Na}^+$  (dashed) in a 2.2 molal NaCl solution with the central force model for water. The average values for the angle are marked on the abscissa.

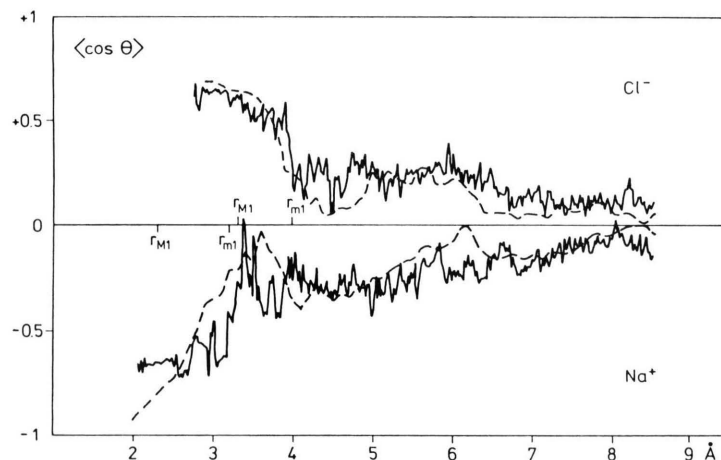


Fig. 8. Average value of  $\cos \theta$  as a function of distance from the chloride (upper part) and the sodium ion.  $\theta$  is defined as the angle between the dipole moment direction of the water molecule and the vector pointing from the oxygen atom towards the center of the ion. The full and dashed lines result from the MD simulation of the 2.2 molal NaCl solution with ST 2 and CF water, respectively.

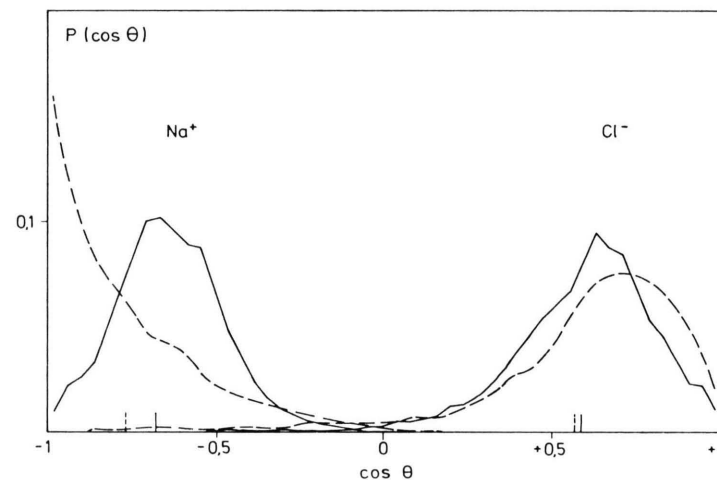


Fig. 9. Angular distributions of the water dipoles in the hydration shells of the sodium and the chloride ion for a 2.2 molal NaCl solution. Full and dashed lines result from the simulation with ST 2 and CF water, respectively. The mean values of  $\cos \theta$  are marked on the abscissa. The distributions are normalized and given in arbitrary units. The definition of  $\theta$  is given in the caption of Figure 8.

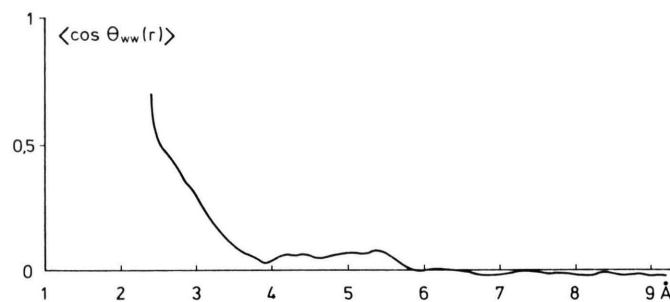


Fig. 10. Average value of  $\cos \theta_{\text{ww}}(r)$  as a function of distance between the oxygen atoms of two water molecules in a 2.2 molal NaCl solution with CF water.  $\theta_{\text{ww}}$  is the angle between the dipole moment vectors of the two water molecules.

detail in Fig. 8 where the average value of  $\cos \theta$  is drawn as a function of the ion-oxygen distance.  $\theta$  is defined as the angle between the dipole moment direction of the water molecule and the vector pointing from the oxygen atom towards the center of the ion. The full and dashed lines result from the simulation of the NaCl solution with ST2 and CF water, respectively. The difference between both kinds of water models seems to be significant only in the case of  $\text{Na}^+$  between 2 and 3.5 Å, the range of the first peak in  $g_{\text{NaO}}(r)$ . The curve for CF water starts with a  $\cos \theta$  value of almost  $-1$  and then increases sharply while in the simulation with ST2 water  $\langle \cos \theta \rangle$  has a constant value of about  $-0.6$  — about half of an tetrahedral angle — in this range. This means that in the case of ST2 water preferentially a lone pair orbital of the water molecules in the hydration shell is directed towards  $\text{Na}^+$ , while in the case of CF water the dipole moment vector of the water molecules and the vector pointing from the oxygen atom to the center of the ion are antiparallel in the immediate neighborhood of  $\text{Na}^+$  and that this preferential orientation decreases rapidly with increasing distance from the ion. This difference in the orientation between the two kinds of water is due to the fact that the lone pair direction is strongly emphasized in the ST2 model through the negative point charge while the repulsive forces exerted from  $\text{Na}^+$  on the two hydrogens tends to a symmetrical arrangement. Obviously the influence of the neighboring water molecules on the orientation becomes with increasing ion-oxygen distance much faster of importance with the CF model than with the ST2 model. For  $\text{Cl}^-$  both curves are rather similar because point charges of similar magnitude are attached to the hydrogen atoms in both water models. This preferential formation of a linear hydrogen bond with the chloride ion has also been found from x-ray and neutron diffraction studies [13, 14]. NMR investigations have led to the same conclusion for the fluoride ion [15]. Experimentally determined orientations of the water molecules in the hydration shells of alkali ions have not been reported.

The different orientational behavior of the water molecules in the hydration shell of  $\text{Na}^+$  in CF and ST2 water becomes even more obvious from the distribution of  $\cos \theta$  as shown for both ions in Figure 9. All water molecules up to the minimum of the RDF's are included in the distributions.

Again the full line is for ST2 and the dashed one for CF water. There is — in agreement with Fig. 8 — no basic difference in the case of  $\text{Cl}^-$ . The average values of  $\cos \theta$  — marked on the abscissa — are nearly the same, the distribution for CF water is slightly flattened with an extended tail at negative values. The distribution in the case of  $\text{Na}^+$  shows for CF water — as expected from Fig. 8 — a strong preference for the orientation where the dipole moment vectors of the water molecules in the hydration shell are antiparallel to the oxygen-ion vector while for ST2 water the distribution shows a preference for the orientation where a lone pair orbital is directed towards the ion. Accordingly, the average value of  $\cos \theta$  is shifted to larger negative values. As no experimental information is available on the orientation of the water molecules in the hydration shell of  $\text{Na}^+$  a judgement on the quality of the two water models is not possible from this point of view.

The average value of the cosine of the angle between the dipole moments of two water molecules in the NaCl solution is shown in Fig. 10 as a function of the distance between the oxygen atoms of the two water molecules. The positive values for  $\langle \cos \theta_{\text{ww}}(r) \rangle$  in the range 4–6 Å reflect the far ranging structure of the water in the solution with CF water which is also demonstrated by the pronounced second maximum and second minimum in  $g_{\text{OO}}(r)$  as drawn in Figure 4. The simulation of the NaCl solution with ST2 water does not show this range of positive values, here  $\langle \cos \theta_{\text{ww}}(r) \rangle \leq 0$  [4]. This different behavior is expressed also in the quantity  $\langle M^2 \rangle / N$ , where  $M$  is defined by

$$M = \sum_i^N m_i$$

and  $m_i$  is the unit vector in the dipole moment direction of water molecule  $i$ . The sum extends over all the  $N=200$  water molecules in the basic cube. An unexpectedly large value for  $\langle M^2 \rangle / N$  of 2.02 has been found for CF water when compared with 0.32 for ST2 water. The value for the  $\text{NH}_4\text{Cl}$  solution with ST2 water was only 0.79 [5] although  $\langle \cos \theta_{\text{ww}}(r) \rangle$  had a similar  $r$  dependence as the one shown in Figure 10.

The structure function calculated from the various RDF's (Figs. 2–6) is compared in Fig. 11 with the ones derived from an x-ray investigation (dotted) [16] and from a MD simulation with ST2

water (dashed) [10]. The double peak in the range of the first maximum of the experimentally determined structure function is reproduced extremely well by the simulation with CF water while the employment of ST2 water results in a single peak. The reason for agreement with CF water and disagreement with ST2 water is the far ranging water-water structure in the case of CF water expressed by the existence of a pronounced second maximum and second minimum in  $g_{OO}(r)$  (Fig. 4). This conclusion has been checked by setting  $g_{OO}(r)=1$  for  $r \geq 4$  Å. In the resulting structure function the double peak was reduced to a single maximum, similar to the one for ST2 water. Additionally, Fig. 11 shows that for  $s > 5$  Å<sup>-1</sup> the experimental structure function is very well reproduced by the simulation with ST2 water while in the case of CF water the agreement is here rather poor. Responsible for this disagreement is the hump at  $s=5.5$  Å<sup>-1</sup> which in turn results from the ion oxygen distances in the hydration shells of Na<sup>+</sup> and Cl<sup>-</sup>. Obviously the CF model of water employed in this simulation leads — at least as far as the structural properties are concerned — to a better description of the solvent in the NaCl solution than

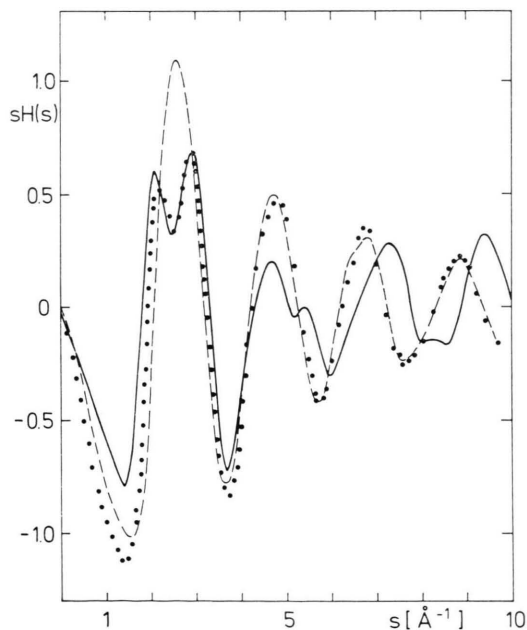


Fig. 11. Comparison of the structure function from an x-ray investigation of a 2 molal NaCl solution (dotted) [16] with the structure functions derived from MD simulations of a 2.2 molal NaCl solution with CF water (full) (this work) and ST 2 water (dashed) [10].

the ST2 model. It is not the CF model which is responsible for the poor agreement for  $s > 5$  Å<sup>-1</sup> but the ion-oxygen pair potentials derived from the ab initio calculations of Kistenmacher, Popkie and Clementi [9].

#### IV. Dynamical Properties

The results presented in this section have to be considered very preliminary as the total simulation extended only over 1.4 psec. As the kinetic energy of the system showed a downward trend and as a rescaling would have raised serious doubts on the usefulness of the dynamical data it did not seem advisable to simulate over a longer period of time. At the other side 1.4 psec are long enough so that the trends indicated can be considered reliable. Unfortunately the dynamical properties of pure CF water in its latest version as employed here have not been calculated by Stillinger and Rahman from their MD run [7] and are therefore not available for comparison. Although the self-diffusion coefficients calculated from this short run for the various subsystems in the NaCl solution are not very reliable, they deviate by less than a factor of two from the experimentally determined ones.

The normalized velocity autocorrelation function for all the oxygens in the 2.2 molal NaCl solution is shown in Figure 12. It is very similar to the one for the water molecules in the 2.2 molal NH<sub>4</sub>Cl solution simulated with ST2 water [5]. The spectral density of the hindered translation of the oxygens calculated by Fourier transformation from the velocity autocorrelation function (Fig. 12) is drawn in Figure 13. The spectrum is very similar to the one of water from the simulation of the NH<sub>4</sub>Cl solution with the ST2 model [5] but shifted by about 10 cm<sup>-1</sup> to higher frequencies. The simulation was not long enough in order to calculate the spectral densities separately for bulk water and hydration water of Na<sup>+</sup> and Cl<sup>-</sup> with a sufficient degree of reliability because a correlation length of 0.7 psec (Fig. 12) was necessary. In the case of the hydrogens — the normalized velocity autocorrelation function is shown in Fig. 14 —, where a correlation length of only 0.15 psec seems to be sufficient, the statistical quality is significantly improved because a much higher number of reference vectors  $v(0)$  can be employed. The differences in the autocorrelation functions between bulk water and hydration water

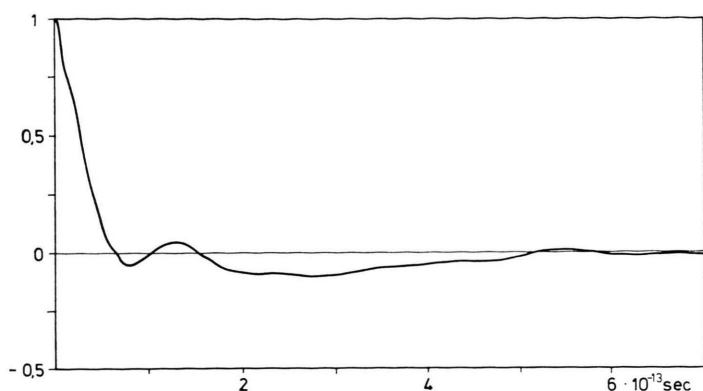


Fig. 12. Normalized velocity autocorrelation function for all oxygens in a 2.2 molal NaCl solution from the simulation with CF water.

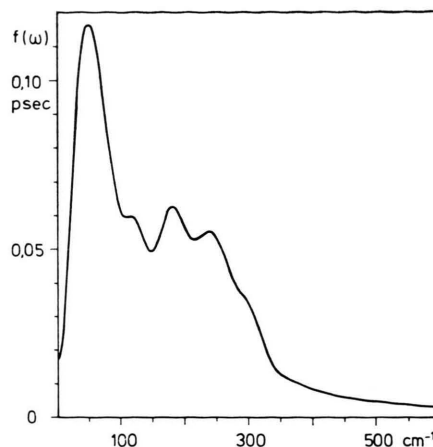


Fig. 13. Spectral density of the hindered translations for all oxygen in the 2.2 molal NaCl solution from the simulation with CF water.

of  $\text{Na}^+$  and  $\text{Cl}^-$  are not pronounced and therefore only the one for all the 400 hydrogens is shown in Figure 14. But the differences between the three kinds of water become obvious in the spectral densities which are drawn for the librational region in Fig. 15, for the bending frequency range in Fig. 16 and for the range of the stretching frequencies in Figure 17.

It has been demonstrated in the preceding paper of this series [5] that the librational band of ST2 water in a 2.2 molal  $\text{NH}_4\text{Cl}$  solution consists mainly of two contributions, one centered around  $400\text{ cm}^{-1}$  and the other one at about  $800\text{ cm}^{-1}$ . The peak at  $400\text{ cm}^{-1}$  has been attributed to librations around the  $x$ - and the  $z$ -axis of a molecule fixed coordinate system (see insertion in Fig. 15) while the one at

$800\text{ cm}^{-1}$  results from the libration around the  $y$ -axis, which has a significantly smaller moment of inertia. Figure 15 shows that the high frequency peak is reduced in its intensity relative to the low

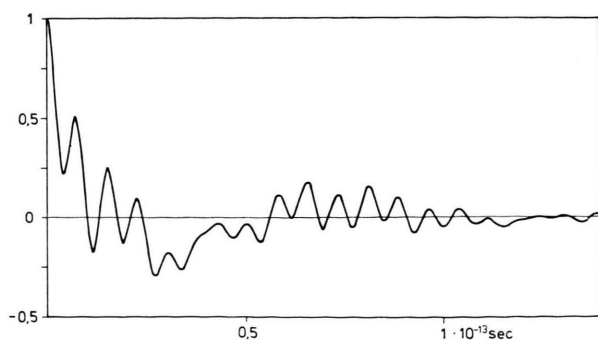


Fig. 14. Normalized velocity autocorrelation function for all hydrogens in a 2.2 molal NaCl solution from a simulation with CF water.

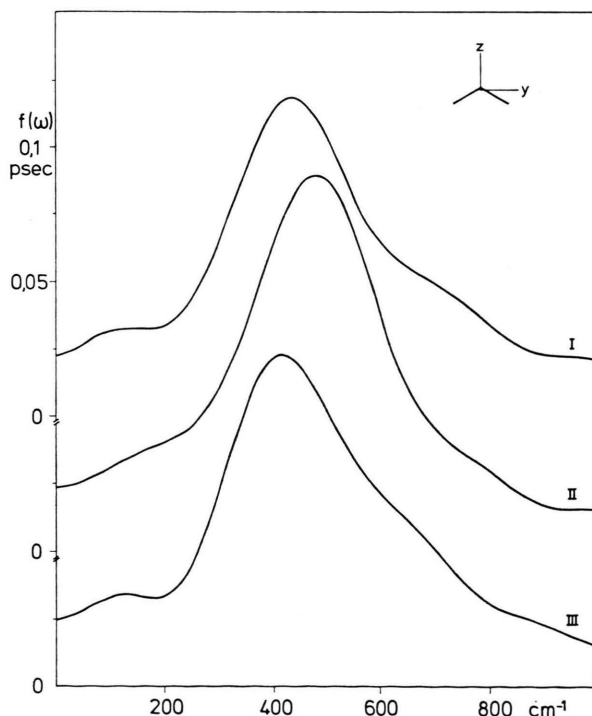


Fig. 15. Spectral densities in the range of the librational frequencies of the water molecules in the 2.2 molal NaCl solution from the simulation with CF water, calculated separately for bulk water (I) and hydration water of  $\text{Na}^+$  (II) and  $\text{Cl}^-$  (III).



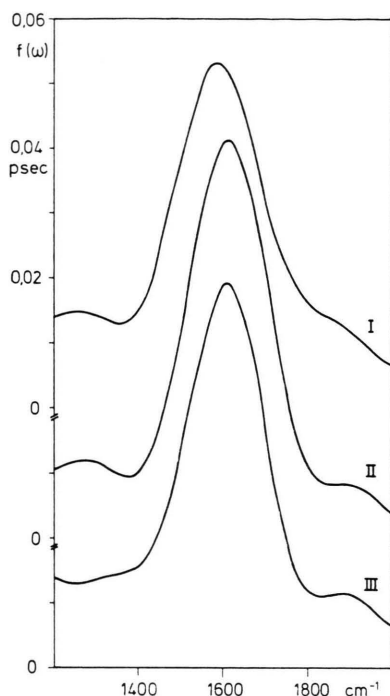


Fig. 16. Spectral densities in the range of the bending vibration of the water molecules in the 2.2 molal NaCl solution from the simulation with CF water, calculated separately for bulk water (I) and hydration water of  $\text{Na}^+$  (II) and  $\text{Cl}^-$  (III).

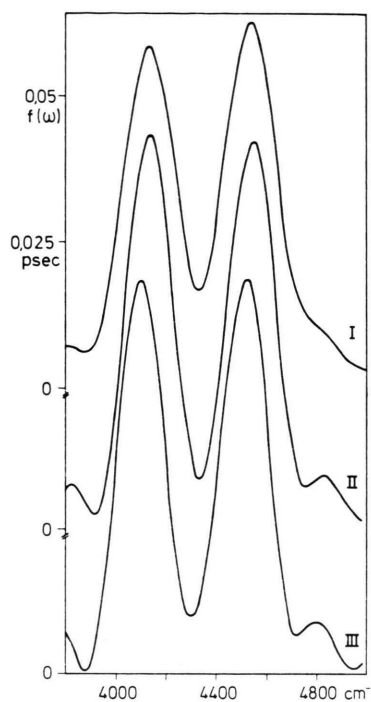


Fig. 17. Spectral densities in the range of the stretching frequencies of the water molecules in the 2.2 molal NaCl solution from the simulation with CF water, calculated separately for bulk water (I) and hydration water of  $\text{Na}^+$  (II) and  $\text{Cl}^-$  (III).

frequency one and shifted to lower frequencies if CF water is employed instead of ST2 water in the simulation of the NaCl solution. The maxima of the spectral densities are positioned at 437, 477 and 422  $\text{cm}^{-1}$  for bulk water (I), hydration water of  $\text{Na}^+$  (II) and  $\text{Cl}^-$  (III), respectively. The significant shift to higher frequencies relative to bulk water in the case of the hydration water of  $\text{Na}^+$  for the librations around the  $x$ - and  $z$ -axis — or at least one of the two axes — indicates a stronger hindrance of the librations not unexpected for a structure making ion as  $\text{Na}^+$ . Accordingly a small shift to lower frequencies results expectedly for the structure breaking ion  $\text{Cl}^-$ . The bands cover the range of librational frequencies measured by far infrared and Raman spectroscopy (see e.g. Refs. [17, 18]) and deduced from model calculations [19].

The spectral densities in the range of the bending frequency (Fig. 16) have their maxima at 1596, 1611 and 1611  $\text{cm}^{-1}$  for bulk water (I), hydration water of  $\text{Na}^+$  (II) and  $\text{Cl}^-$  (III), respectively. The result that the positions of the maxima of both kinds of hydration water are the same but shifted slightly

to higher frequencies compared with bulk water is in accordance with the distributions of the HOH angle (Figure 7). The distributions for the two kinds of hydration water are very similar and the average value of the HOH angle is slightly smaller than for bulk water, which means an increase in the force constant for the bending vibration and consequently higher frequencies. Infrared and Raman spectroscopic investigations indicate no or only a small shift to lower frequencies for the bending vibration in going from pure water to a concentrated NaCl solution (see e.g. [17, 18]). These experimental results can not be compared with results derived from this simulation as the spectral density for pure CF water has not been calculated by Stillinger and Rahman [7] and as bulk water in a 2.2 molal NaCl solution does not show necessarily the properties of pure water (see discussion in [5]). The experimentally determined spectral density for pure water centered at 1645  $\text{cm}^{-1}$  [18] can, of course, not be employed for comparison as it can not be expected that the CF model leads to the same value for pure water.

Strong deficiencies of this version of the CF model become obvious in the range of the stretching vibrations as shown in Fig. 17, where asymmetric and symmetric stretching vibrations are well separated at about 4100 and 4550  $\text{cm}^{-1}$  while from infrared and Raman investigations a broad band between 3200–3700  $\text{cm}^{-1}$  results. In spite of this discrepancy the relative shift between the three kinds of water in the NaCl solution might be significant. The positions of the maximum of  $\nu_1$  are located at 4535, 4548 and 4523 and of  $\nu_3$  at 4133, 4133 and 4095 for bulk water (I) hydration water of  $\text{Na}^+$  (II) and  $\text{Cl}^-$  (III), respectively.  $\nu_1$  is shifted relative to bulk water to a higher frequency for the structure making and a lower frequency for the structure breaking ion, while for  $\nu_3$  only the hydration water of  $\text{Cl}^-$  shows a shift to lower frequencies. Infrared measurements indicate shifts to higher frequencies by going from pure water to a 2.5 molal NaCl solution of 20 and 40  $\text{cm}^{-1}$  for  $\nu_1$  and  $\nu_3$ , respectively [17].

The residence time of the water molecules in the hydration shells of  $\text{Na}^+$  and  $\text{Cl}^-$  has been calculated from the normalized autocorrelation function of the hydrate vector  $\mathbf{h}(t)$ . This vector has 200 components where each component represents one of the 200 water molecules in the basic periodic cube. The components have the values 1 if a water molecule belongs to the hydration shell of one of the eight ions of the same kind and zero if not. The resulting normalized autocorrelation function  $\langle \mathbf{h}(0) \mathbf{h}(t) \rangle / \langle \mathbf{h}(0)^2 \rangle$  for  $\text{Cl}^-$  is shown in Figure 18.

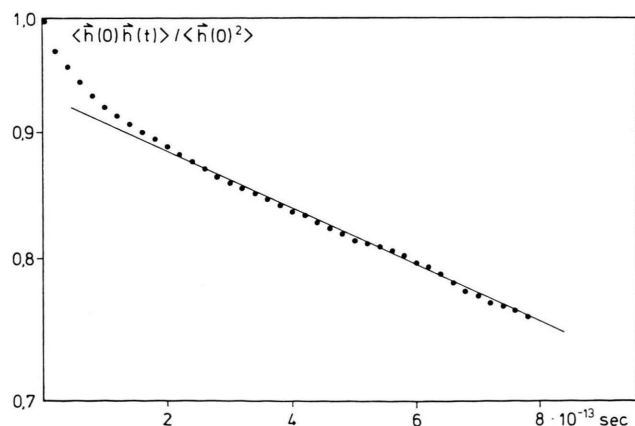


Fig. 18. Normalized autocorrelation function of the hydrate vector for  $\text{Cl}^-$  from a simulation of a 2.2 molal NaCl solution with the central force model for water.

From the slope for  $t > 0.2$  psec a residence time of 3.8 psec results. The residence time for water molecules in the hydration shell of  $\text{Na}^+$  is significantly longer. The total simulation time of 1.4 psec is too short to calculate the residence time for  $\text{Na}^+$  with sufficient accuracy.

The reorientation time of the unit vector in the dipole moment direction of a water molecule  $\boldsymbol{\mu}(t)$  has been calculated from the simulation for the water molecules in the 2.2 molal NaCl solution by

$$\text{MD}\tau_{1D} = \int_0^{\infty} \Gamma_{1D}(t) dt$$

where

$$\Gamma_{1D}(t) = \langle \boldsymbol{\mu}(0) \boldsymbol{\mu}(t) \rangle.$$

$\Gamma_{1D}$  is shown in Figure 19. Up to about 0.1 psec the librational motions of the water molecules (Fig. 15) determine  $\Gamma_{1D}$ . In the ranges  $0.1 < t < 0.4$  psec and  $t > 0.6$  psec nearly an exponential decay is found with time constants of about 4 and 15 psec, respectively. Dielectric measurements of a NaCl solution show that the frequency dependence of the complex permittivity has to be described by a distribution of reorientation times. The extrapolation of the concentration dependence results for a 2.2 molal NaCl solution in a macroscopic  $\exp\tau_{1D} \approx 7.0$  psec [20]. Assuming a distribution of reorientation times between 4 and 15 psec from the simulation an average reorientation time of about 7.7 psec follows in reasonable agreement with the experimental result.

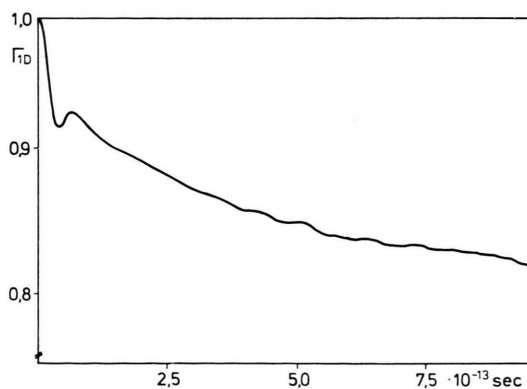


Fig. 19. Normalized autocorrelation function for the water dipoles in a 2.2 molal NaCl solution with the central force model for water.

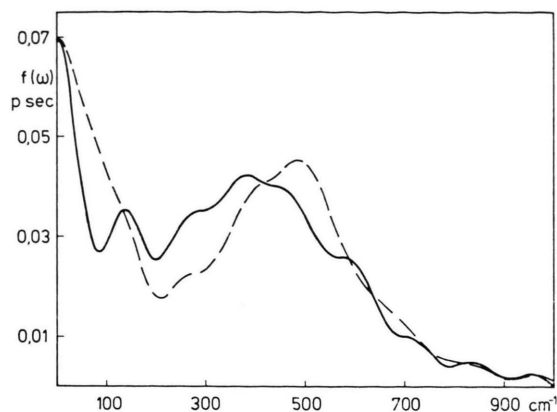


Fig. 20. Result of the Fourier transformation of the autocorrelation functions of the dipole moment unit vector for the hydration water of  $\text{Na}^+$  (dashed) and  $\text{Cl}^-$  (full) after subtraction of the exponential term, from the simulation of a 2.2 molal NaCl solution with the central force model for water.

Finally it is demonstrated that  $\Gamma_{1D}$  in the range  $t < 0.1$  psec reflects the librational behavior of the water molecules. From the autocorrelation functions of the dipole moment unit vector for the hydration water of  $\text{Na}^+$  and  $\text{Cl}^-$  —  $\Gamma_{1D}^+$  and  $\Gamma_{1D}^-$  — the exponential term has been subtracted and the remaining contribution subjected to a Fourier transformation. The results are shown in Fig. 20. In spite of the fact that the statistical uncertainties in  $\Gamma_{1D}^+$  and  $\Gamma_{1D}^-$  are significantly larger than in  $\Gamma_{1D}$  because of the smaller number of water molecules involved, the comparison of Fig. 20 with Fig. 15 shows that the main features of the librational motions are reproduced.

#### Acknowledgement

The authors are grateful to Dr. L. Schäfer for supplying his predictor-corrector program and to Dr. A. Geiger for the Ewald routine. Helpful discussions with Dr. Gy. Szász and financial support

by Deutsche Forschungsgemeinschaft are gratefully acknowledged.

#### Appendix

The pair potentials employed in the MD simulation of the 2.2 molal NaCl solution are given in Eqs. (A.1)–(A.10) with  $r$  in Å and  $V$  in units of  $10^{-12}$  erg. The ion-water pair potentials for the energetically most favorable orientations are drawn, additionally, in Figure 1.

$$V_{\text{HH}}(r) = 2.509/r + 1.251/\{1 + \exp[40(r - 2.05)]\} - 1.181 \exp[-7.622(r - 1.4525)^2]; \quad (\text{A.1})$$

$$V_{\text{OH}}(r) = -5.019/r + 0.433/r^{9.2} - 0.694/\{1 + \exp[40(r - 1.05)]\} - 0.278/\{1 + \exp[5.493(r - 2.2)]\}; \quad (\text{A.2})$$

$$V_{\text{OO}}(r) = 10.04/r + 1858/r^{8.86} - 1.736 \cdot 10^{-2} \cdot \{\exp[-4(r - 3.4)^2] + \exp[-1.5(r - 4.5)^2]\}; \quad (\text{A.3})$$

$$V_{\text{NaNa}}(r) = 23.06/r + 2.375 \cdot 10^{-2} \cdot [(2.73/r)^{12} - (2.73/r)^6]; \quad (\text{A.4})$$

$$V_{\text{NaCl}}(r) = -23.06/r + 1.133 \cdot 10^{-2} \cdot [(3.87/r)^{12} - (3.87/r)^6]; \quad (\text{A.5})$$

$$V_{\text{ClCl}}(r) = 23.06/r + 1.115 \cdot 10^{-2} \cdot [(4.86/r)^{12} - (4.86/r)^6]; \quad (\text{A.6})$$

$$V_{\text{NaO}}(r) = -15.22/r - 2.55/r^2 + 8125 \exp(-4.526r); \quad (\text{A.7})$$

$$V_{\text{NaH}}(r) = 7.61/r + 0.52/r^2 + 6921 \exp(-7.07r); \quad (\text{A.8})$$

$$V_{\text{ClO}}(r) = 15.22/r - 1.81 \cdot 10^{-2}/r^2 + 6230 \exp(-3.28r); \quad (\text{A.9})$$

$$V_{\text{ClH}}(r) = -7.61/r - 0.28/r^2 + 181.9 \exp(-3.314r). \quad (\text{A.10})$$

- [1] D. L. Beveridge, M. Mezei, S. Swaminathan, and S. W. Harrison, ACS Symposium Series **86**, 191 (1978).
- [2] H. Kistenmacher, H. Popkie, and E. Clementi, J. Chem. Phys. **61**, 799 (1974).
- [3] O. Matsuoka, E. Clementi, and M. Yoshimine, J. Chem. Phys. **64**, 1351 (1976).
- [4] K. Heinzinger and P. C. Vogel, Z. Naturforsch. **31a**, 463 (1976).
- [5] Gy. I. Szász and K. Heinzinger, Z. Naturforsch. **34a**, 840 (1979); Gy. I. Szász, W. O. Riede, and K. Heinzinger, Z. Naturforsch. **34a**, 1083 (1979).
- [6] F. H. Stillinger and A. Rahman, J. Chem. Phys. **60**, 1545 (1974).

- [7] F. H. Stillinger and A. Rahman, J. Chem. Phys. **68**, 666 (1978).
- [8] H. L. Lemberg and F. H. Stillinger, J. Chem. Phys. **62**, 1677 (1975).
- [9] H. Kistenmacher, H. Popkie, and E. Clementi, J. Chem. Phys. **58**, 1689 (1973) (a); 5627 (1973) (b); **59**, 5842 (1973) (c).
- [10] G. Pálinkás, W. O. Riede, and K. Heinzinger, Z. Naturforsch. **32a**, 1137 (1977).
- [11] L. Schäfer and A. Klemm, Z. Naturforsch. **31a**, 1068 (1976).
- [12] A. Rahman, F. H. Stillinger, and H. L. Lemberg, J. Chem. Phys. **63**, 5223 (1975).

- [13] A. H. Narten, F. Vaslow, and H. A. Levy, *J. Chem. Phys.* **58**, 5017 (1973).
- [14] A. K. Soper, G. W. Neilson, J. E. Enderby, and R. A. Howe, *J. Phys. C.: Solid St. Phys.* **10**, 1793 (1977).
- [15] H. G. Hertz and C. Rädle, *Ber. Bunsenges.* **77**, 521 (1973).
- [16] G. Pálincás, T. Radnai, and F. Hajdu, *Z. Naturforsch.* **35a**, Heft 1 (1980).
- [17] R. E. Verrall, in: *Water, a Comprehensive Treatise* (F. Franks, ed.), Plenum Press, New York 1973, Vol. 3.
- [18] T. H. Lilley, in [17].
- [19] B. Curnutte and D. Williams, in: *Structure of Water and Aqueous Solutions* (W. A. P. Luck, ed.), Verlag Chemie, Weinheim 1974.
- [20] R. Pottel in [17].